Available online at www.sciencedirect.com
ScienceDirect
Computational Materials Science 39 (2007) 55–64
COMPUTATIONAL MATERIALS SCIENCE
www.elsevier.com/locate/commatsci

Modelling of creep-fatigue in containers during aluminium and copper extrusion

C. Sommitsch [a,b,*], R. Sievert [c], T. Wlanis [a], B. Günther [c], V. Wieser [d]

[a] Chair of Metal Forming, University of Leoben, Franz-Josef-Strasse 18, 8700 Leoben, Austria
[b] Christian Doppler Laboratory for Materials Modelling and Simulation, University of Leoben, Franz-Josef-Strasse 18, 8700 Leoben, Austria
[c] Federal Institute for Materials Research and Testing (BAM), Division V.2 Mechanical Behaviour of Materials, Unter den Eichen 87, 12200 Berlin, Germany
[d] Böhler Edelstahl GmbH, Mariazellerstrasse 25, 8605 Kapfenberg, Austria

Received 30 September 2005; received in revised form 19 December 2005; accepted 29 March 2006

Abstract

During hot extrusion of aluminium alloys, extrusion dies experience cyclic temperature changes as well as multiaxial loadings. To improve the service life of the dies, cleaner and high hot strength materials are designed as well as an optimised process control is performed. For the improvement of the process guiding and a comparison of lifetime behaviour of different hot work tool steels, modelling and simulation are appropriate means. The extrusion process has been simulated using the FE-program Deform to find the stress and temperature history at the inner diameter of the liner, i.e. the boundary conditions for the subsequent cyclic simulation of the container during service. Inelastic constitutive equations have been implemented into Abaqus Standard to describe strain hardening and time recovery effects. They include the Norton viscoplastic flow rule, thermo-mechanical isotropic hardening and two non-linear kinematic hardening laws. A damage-rate model predicts failure and thus the lifetime of the container. The procedure for the identification of material parameters for both the constitutive and the damage model is described in detail for the hot work tool steel Böhler W400 VMR (EN 1.2343).

Keywords: Extrusion; Hot work tool steels; Creep-fatigue; Lifetime; Damage

1. Introduction

Extrusion tools exhibit a complex strain-time pattern under a variety of cyclic loading conditions and thus are prone to failure by creep-fatigue interactions [1,2]. Elevated temperature failure by creep-fatigue processes is time dependent and often involves deformation path dependent interactions of cracks with grain boundary cavities [3]. The extrusion industry tries to accelerate the process by increasing the billet temperature and/or by accelerating the press speed that raise the loading of the tools. On the other side the tool steel producers develop enhanced more homogeneous and cleaner materials in order to increase tools lifetime. Finite element simulation of the extrusion process to get the temperature and stress evolution in the tools, coupled with constitutive equations as well as lifetime consumption models in order to calculate both the inelastic strains and the tools lifetime, help to optimise the extrusion process and to compare the operating times of different hot work tool steels.

Viscoplastic constitutive models have been developed in the past to take into account the inelastic behaviour of the material during creep-fatigue loads, see, e.g., [4–6]. In the present study the Chaboche model has been selected and calibrated to the material response of Böhler W400 VMR (EN 1.2343) hot work tool steel between 470 °C and 590 °C. To extend the prediction capability of Chaboche's

* Corresponding author. Address: Chair of Metal Forming, University of Leoben, Franz-Josef-Strasse 18, 8700 Leoben, Austria. Tel.: +43 3842 402 5605; fax: +43 3842 402 5602.
E-mail address: christof.sommitsch@mu-leoben.at (C. Sommitsch).

0927-0256/$ - see front matter © 2006 Elsevier B.V. All rights reserved.
doi:10.1016/j.commatsci.2006.03.024

model for non-isothermal processes a certain temperature-rate term has been added to the isotropic hardening rule [7]. Additionally, a creep-fatigue lifetime rule for complex processes is investigated that is independent of single loading parameters, like stress or strain ranges or corresponding maxima, for the description of an entire cycle. Instead this rule evaluates the total damage in each time increment and accumulates that to the lifetime consumption.

The present paper shows the development of temperatures, stresses and lifetime consumption in the liner of a 2-part container over several extrusion cycles until the process reaches a steady state. Two extrusion temperatures that should reproduce both aluminium and copper extrusion have been chosen in order to compare temperature's impact on tools lifetime.

2. Modelling and simulation

The numerical extrusion simulation consists of the plastic simulation of the billet extrusion with rigid tools as well as of the subsequent simulation of several cycles of the same process, only considering the elastic 2-part container and using the time dependent temperature and radial stress boundary conditions at the inner diameter of the liner.

2.1. Extrusion model

To predict damage, the accurate knowledge of the unsteady local thermal and mechanical loading within one cycle on the inner diameter of the liner is of particular importance. Hence the thermo-mechanical load of a container during extrusion of a billet has been analysed by means of the finite element method. Since the container assembly is symmetrical, a 2D axi-symmetric model of the container has been used (Fig. 1a). The die, ram and die-holder have been assumed to be rigid. The temperature-dependent thermo-physical material properties (thermal expansion, thermal conductivity, heat capacity and emissivity) for the liner made of Böhler W400 VMR and for the mantle made of Böhler W300 ESR have been taken from existing material databases. The length L, inner diameter D_i and outer diameter D_o of the liner, mantle and billet, respectively, have been assumed to be:

Liner: $L = 760$ mm; $D_i = 240$ mm, $D_o = 360$ mm.
Mantle: $L = 755$ mm; $D_i = 360$ mm; $D_o = 820$ mm.
Billet: $L = 650$ mm; $D = 234$ mm.

The shrink-fitting of the mantle has been simulated by a shrinkage of 0.8‰. For the billet material, electro copper has been chosen with an initial temperature of 780 °C. For the sake of simplicity, for the simulation of aluminium extrusion, the temperature boundary conditions has been reduced by a constant factor related to the copper extrusion, while the radial stress boundary conditions has not been changed. This can be done because the radial stress, which acts on the inner tool surfaces, e.g., on the liner, during pressing is in the same range for the extrusion of hard extrudable aluminium alloys and of medium extrudable copper alloys [8].

The necessary contact conditions (friction, interface heat transfer coefficient) between liner and mantle and the boundary conditions (convection coefficient, emissivity) have been described using existing data. Fig. 1b shows the von Mises stress distribution in the container during the first extrusion cycle after 15 s. The cause of this non-uniform stress distribution is the complex load case, which consists of

- shrinkage stresses after shrink-fitting,
- axial stresses as a result of pressing on the container against the die-holder,

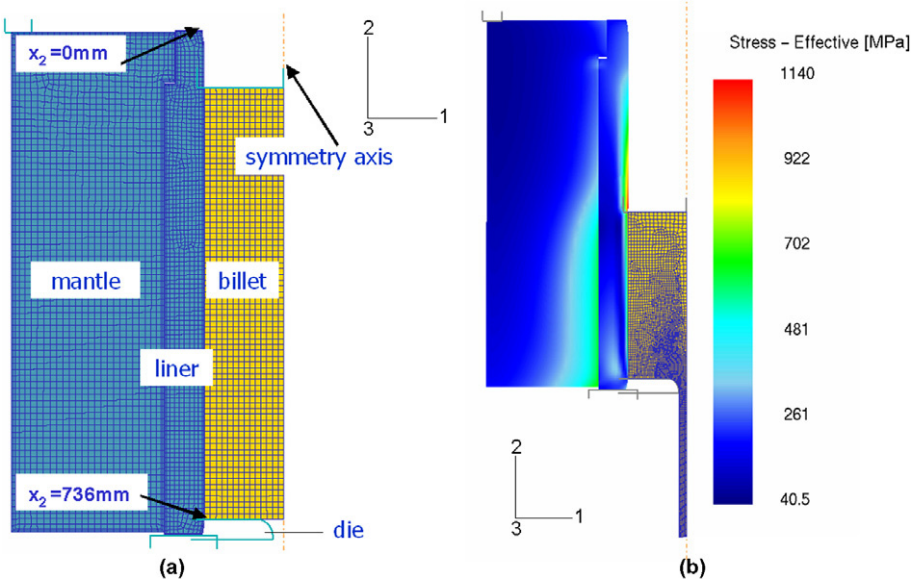

Fig. 1. Extrusion model (a) and von Mises stress distribution after 15 s during the first extrusion cycle (b); DEFORM 2D simulation.

- thermal stresses due to the pre-heating to working temperature and the temperature rise during an extrusion cycle,
- axial stresses and radial compressive stresses during one extrusion cycle at the contact surface between billet and inner diameter of the liner.

The simulated processes are listed below:

- shrink-fitting of the mantle (0.8‰),
- pre-heating of the container to a working temperature of 400 °C,
- pressing on the container against the die-holder,
- forward extrusion of the billet with a ram speed of 20 mm/s.

From the development of the radial stress at the inner diameter of the liner the non-uniform load state of the container can be derived (Fig. 2a and b). An adequate high number of extrusion cycles has to be taken into account in order to calculate the steady state operating condition and thus the time and axial position dependent boundary conditions for the container. These boundary conditions have been used for a minimisation of calculation time, which is described in the following.

2.2. Model of cyclic container loads

For the calculation of the cyclic temperature and stress evolution in the container, Abaqus Standart v.6.5-1 FEM calculations have been conducted with elastic liner and mantle. Since the container assembly is symmetrical, an axisymmetric model of the container was used. First, the shrink-fitting of mantle and liner (0.8‰ of the internal diameter of the container) and the pre-heating to working temperature (400 °C) have been simulated. Within each extrusion cycle, both the heat of the billet and the applied radial stresses have been defined by the above described boundary condition at the inner diameter of the liner. Fig. 3 shows the temperature and radial stress boundary condition as well as the procedure of applying time dependent stresses and temperatures. Fifteen extrusion cycles have been simulated to reach quasi-stationary operating conditions. Fig. 4 displays both the temperature (a) and stress distribution (b) at the end of the first extrusion cycle for aluminium extrusion. The maximum temperature (ca. 500 °C and 600 °C for aluminium and copper extrusion, respectively) appears at the inner diameter of the liner near the die where the contact time with the billet during extrusion has its maximum, however the maximum Mises equivalent stress has its maximum slightly above that region of maximum temperature.

2.3. Model for the deformation behaviour

For this investigation a viscoplastic model is used according to Chaboche [6], where the total strain e is taken to be composed of elastic e_e, thermal e_{th} as well as inelastic e_{in} parts

$$e = e_e(r) + e_{in} + e_{th}(T), \quad e_{th}(T_0) = e_{th}(T_1) \tag{1}$$

and the Hookean law is given by

$$r = 2Ge_e^0 + \frac{E}{3(1-2m)}\mathrm{tr}e_e\mathbf{1}; \tag{2}$$

with G denotes the shear modulus, E the Young's modulus, mthe Poisson's ratio and the deviator of the elastic strain tensor e_e^0

$$e_e^0 := e_e - \frac{1}{3}\mathrm{tr}e_e\mathbf{1}; \quad \mathrm{tr}e_e := e_{e;1} + e_{e;2} + e_{e;3}: \tag{3}$$

For the lifetime prediction of highly stressed extrusion tools during service, taking into account the inelastic strain rate during a cycle, it is necessary to be able to assess the inelastic stress–strain response of the material [9]. The influence of the thermo-mechanical history on the current stress–strain behaviour can be described with internal (non-measurable) variables, beside the measurable (external) variables of deformation, time, temperature and stress [5]. The evolution equations for the internal variables are given by flow and hardening rules. In viscoplastic, i.e. unified inelastic, models, creep and plasticity are covered within a single inelastic strain variable in order to describe creep-plasticity interaction. The flow rule, i.e. the evolution equation for the inelastic strain is [6]

$$\dot{e}_{in} = \frac{3}{2}\left\langle\frac{J_2(\mathbf{S}-\mathbf{X})-(k+R)}{K}\right\rangle^n \frac{\mathbf{S}-\mathbf{X}}{J_2(\mathbf{S}-\mathbf{X})}; \quad \langle y\rangle := \begin{cases} y; & \text{if } y > 0 \\ 0; & \text{otherwise} \end{cases} \tag{4}$$

with the applied stress deviator $\mathbf{S}$

$$\mathbf{S} := r - \frac{1}{3}\mathrm{tr}r\mathbf{1}; \quad J_2(\mathbf{A}) := \sqrt{\frac{3}{2}\mathbf{A}:\mathbf{A}}; \tag{5}$$

specifying k as the initial elastic limit, R as the increase of the elastic limit due to hardening, $\mathbf{X}$ as the internal back stress tensor, describing kinematic hardening and K as a material parameter. Olschewski et al. [7] have proposed a certain type of a thermal–mechanical evolution equation for the isotropic hardening variable $R = Q(T)r$ in order to describe non-isothermal material behaviour, T denotes the temperature:

$$\dot{R} = Q\dot{r} + \frac{R}{Q}\frac{dQ}{dT}\dot{T} \tag{6}$$

with Q as the saturation parameter of R at isothermal loading and r as the related isotropic hardening variable with the evolution equation

$$\dot{r} = b\left(1 - \frac{R}{Q}\right)\dot{p} - f\left(\frac{R}{Q}\right)^s; \quad r(t=0) = 0; \quad \dot{p} := \sqrt{\frac{2}{3}}\|\dot{e}_{in}\| \tag{7}$$

where b, f and s are material parameters adapting the isotropic hardening and static recovering, respectively, and $\dot{p}$ is the inelastic Mises equivalent strain-rate.

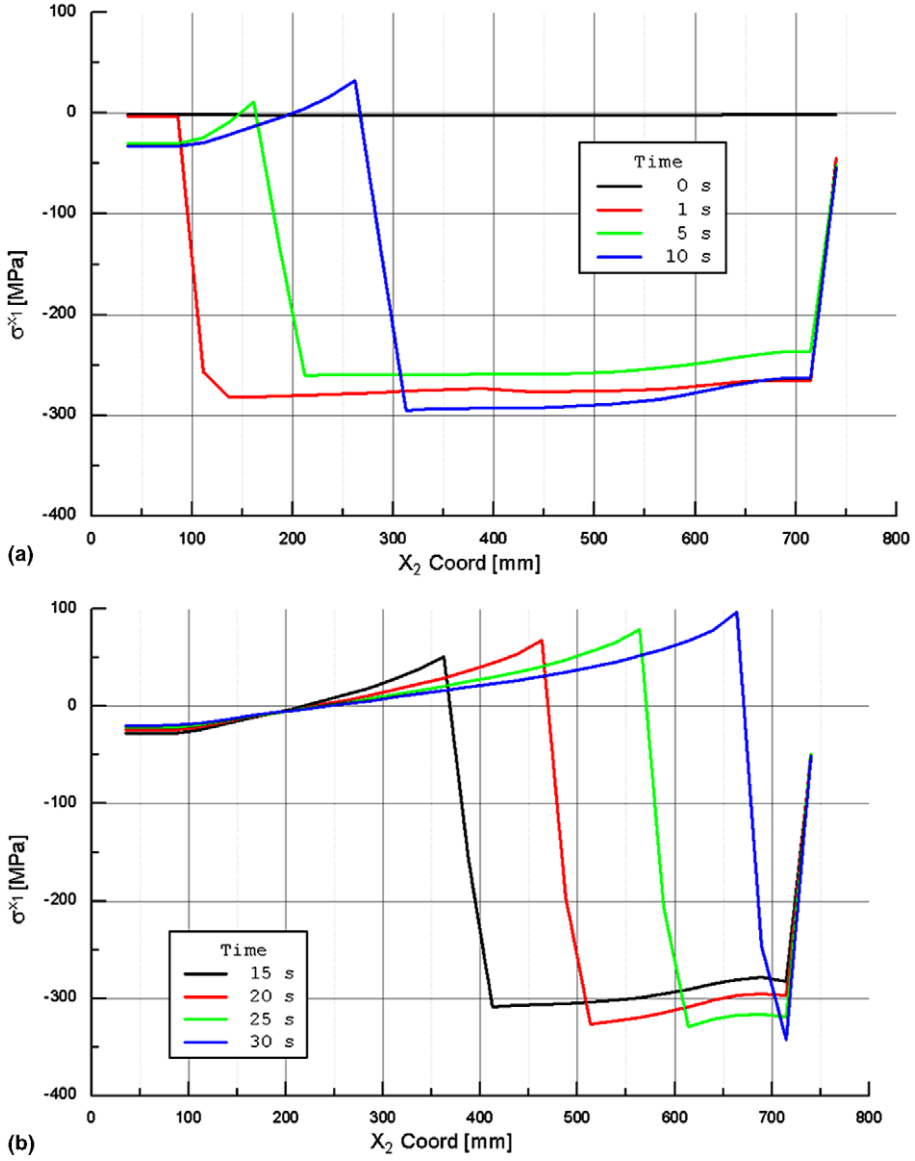

Fig. 2. Radial stress at the inner diameter of the liner during one extrusion cycle after 1, 5 and 10 s (a); and during 15, 20, 25 and 30 s (b), respectively.

The rate equations for the kinematic hardening variables obey a unique format. The back stress $\mathbf{X}$ is decomposed into independent variables $\mathbf{X}_i$, each of them being of the same rule. As shown in previous studies (e.g., Watanabe and Atluri [10]), two or three of such variables are sufficient to describe, very correctly, the real materials. In this work two independent variables have been chosen

$$\mathbf{X} = \mathbf{X}_1 + \mathbf{X}_2; \qquad \mathbf{X}_i = \frac{2}{3} a_i(T)\boldsymbol{\alpha}_i; \quad i = 1; 2; \tag{8}$$

where $a_i(T)$ are saturation parameters of the internal back-stresses $\mathbf{X}_i$, and a_i are related kinematic hardening variables:

$$\dot{\boldsymbol{\alpha}}_i = c_i \dot{\boldsymbol{\varepsilon}}_{in} - \frac{3}{2} c_i \frac{\mathbf{X}_i}{a_i} \dot{p} - \frac{3}{2} \frac{d_i}{a_i} \left[\frac{J_2(\mathbf{X}_i)}{a_i} \right]^{m_i} \frac{\mathbf{X}_i}{J_2(\mathbf{X}_i)}; \quad a_i(t=0) = 0 \tag{9}$$

with c_i, d_i and m_i as material parameters defining the kinematic hardening and the static recovering, respectively.

The related hardening variables r and a_i are describing the degree of hardening, that corresponds in the material structure to the accumulation of immobile dislocations (compare, e.g., Ilschner [11]) and that causes certain internal stresses $k + R$ and $\mathbf{X}_i$, respectively, at a certain temperature. For example, the isotropic variable r tends, at negligible static recovery, according to Eq. (7) for any temperature to its saturation value 1. Something similar is the case for the kinematic variables a_i according to Eq. (9) at proportional loading. Thus, the internal stresses $k + R$ and $\mathbf{X}_i$ vary at temperature changes according to Eqs. (6) and (8) at most to their saturation levels (Q and $2/3\ a_i$) at the current temperature (compare Olschewski et al. [7] and Frenz et al. [9]).

All thermo-physical and material parameters are temperature-dependent and have been determined for temperatures in the range of 470 °C–590 °C with 30 °C temperature steps. For a reduction of the number of parameters,

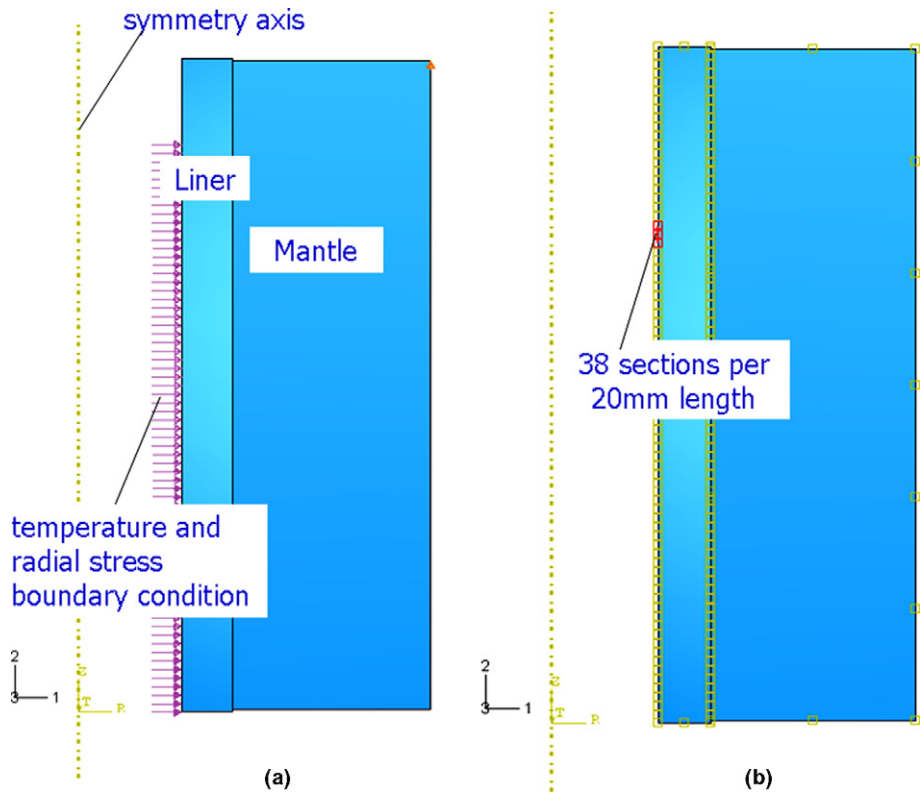

Fig. 3. Temperature and radial stress boundary condition, predicted by the previous DEFORM 2D simulation (a). The mantle consists of 1600 and the liner of 7600 CAX4RT elements. The minimum element size is 1.4 mm at the inner diameter of the liner. The time dependent boundary condition at the inner diameter of the liner is applied by 38 sections per 20 mm length (b).

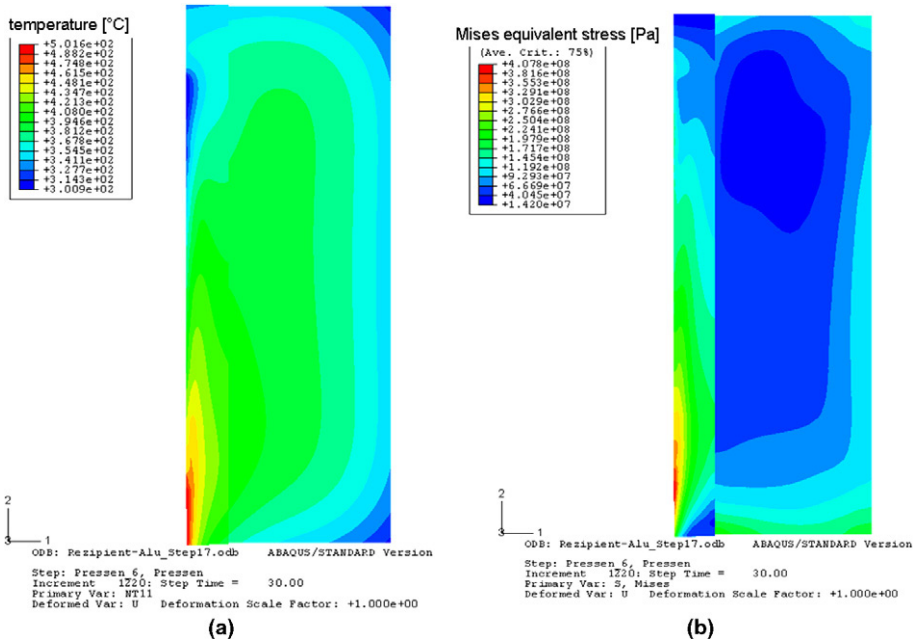

Fig. 4. Temperature in °C (a) and Mises equivalent stress in Pa (b) distribution in liner and mantel at the end of the first aluminium extrusion cycle.

the material parameters of the thermal, so-called static, recovery of the internal back-stresses $\mathbf{X}_i$ are set equal: $d_1 = d_2 =: d$, $m_1 = m_2 =: m$. With respect to the number of material parameters to be determined it can be said, that as much material parameters can be identified as material phenomena can be observed in the experiments. Such phenomena of the hardening and recovery behaviour are listed in the following together with the corresponding

material parameters to be identified especially from these phenomena, and that in the sequence of the parameter determination:

I. The *primary rate-dependence* (n, K) appears in the stress differences at different inelastic strain-rates at the same hardening state without any time-dependent recovery effects.
II. The *initial yield strength* $R_{p0.005}$ corresponds approximately to the initial radius (k) of the elastic range plus the viscous stress $r_v(\dot{\underline{e}}_{in})$, the latter represents the rate-dependence of the yield strength:

$$R_{p0.005} = k + r_v(\dot{\underline{e}}_{in}), \quad r_v(\dot{\underline{e}}_{in}) = K|\dot{\underline{e}}_{in}|^{1/n} \qquad (10)$$

III. The *isotropic hardening* (Q, b) appears in the cyclic development of the diameter of the quasi-elastic ranges in the hysteresis loops at unloading. This diameter minus the viscous stresses gives twice the radius $k+R$ of the elastic range of the model (Fig. 5).
IV. The *kinematic hardening* (c_i, a_i) describes the midpoint of the elastic range observable by the quasi-elastic ranges in the hysteresis loops. Additionally, kinematic hardening is also present in the flow curve of a tensile test.
V. The *static recovery* $(d, m; f, s)$ appears in long-term stress relaxation and in steady-state creep-rates.

In order to determine the parameters of the primary rate-dependence as well as of the static recovery, strain-controlled tensile tests with subsequent strain hold-time, i.e. stress relaxation, periods of several hours (up to 40 h) have been performed at different temperatures (compare Krempl [12]). During relaxation several magnitudes of the inelastic strain-rate (creep rates) occur which decrease (down to $10^{-8}\ s^{-1}$) with the decreasing magnitude of the stress-rate. The simulation of the material response of the investigated hot working steel Böhler W400 VMR in such a relaxation test is represented in Fig. 6. For the determination of the hardening parameters, hysteresis loops of strain-controlled cyclic tests without hold-times have been evaluated. For verification, the simulation of the hysteresis loops with strain hold-times is given in Fig. 7.

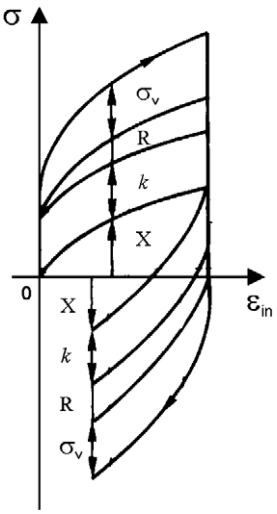

Fig. 5. Decomposition of stress into internal and viscous parts for cyclic loading (after Lemaitre and Chaboche [5]).

2.4. A lifetime rule for complex processes

Cyclically loaded structures suffer a fatigue failure. Fatigue lifetime means in a macroscopic model the initiation of a macro-crack (typically a fraction of millimetre). Fatigue lifetime rules are usually formulated on the basis of mean quantities of a cycle, like stress or strain ranges (see, e.g., Chaboche and Gallerneau [13]). In contrast, time incremental lifetime rules ([3,14–17]) evaluate the total damage in each time increment and, thus, can be applied also to complex multiaxial loading paths, for which the definition of a single loading parameter describing the entire cycle could be difficult. Furthermore, a time incremental lifetime rule can easily be implemented in a material sub-routine for finite element analysis of structures just as an evolution equation for an additional internal variable, the lifetime

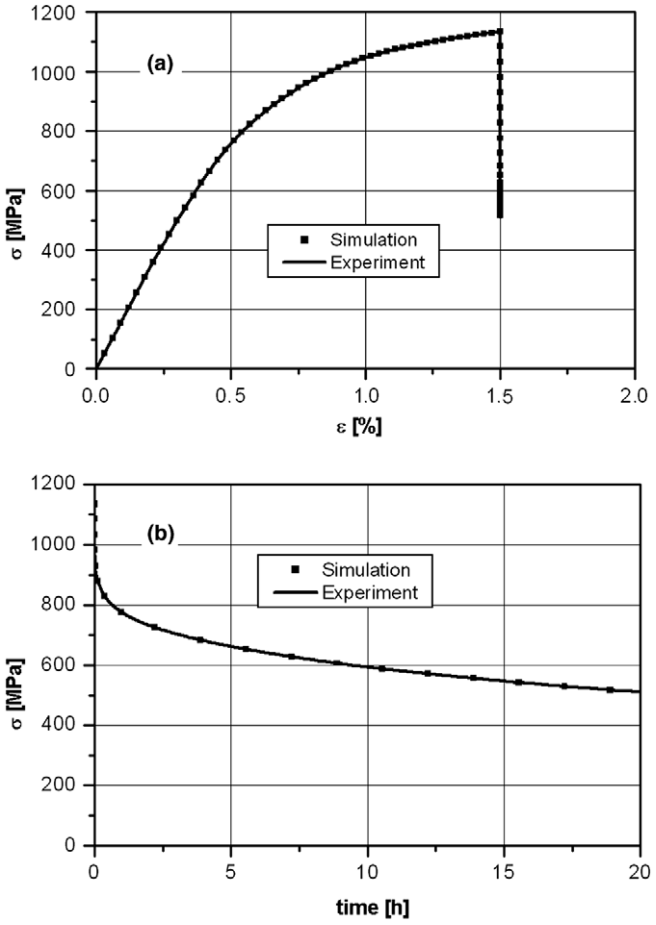

Fig. 6. Simulation of the relaxation behaviour at 560 °C used for the calibration of the model: stress vs. strain with a strain-rate of $10^{-3}\ s^{-1}$ up to the strain-hold (a); stress vs. time (b).

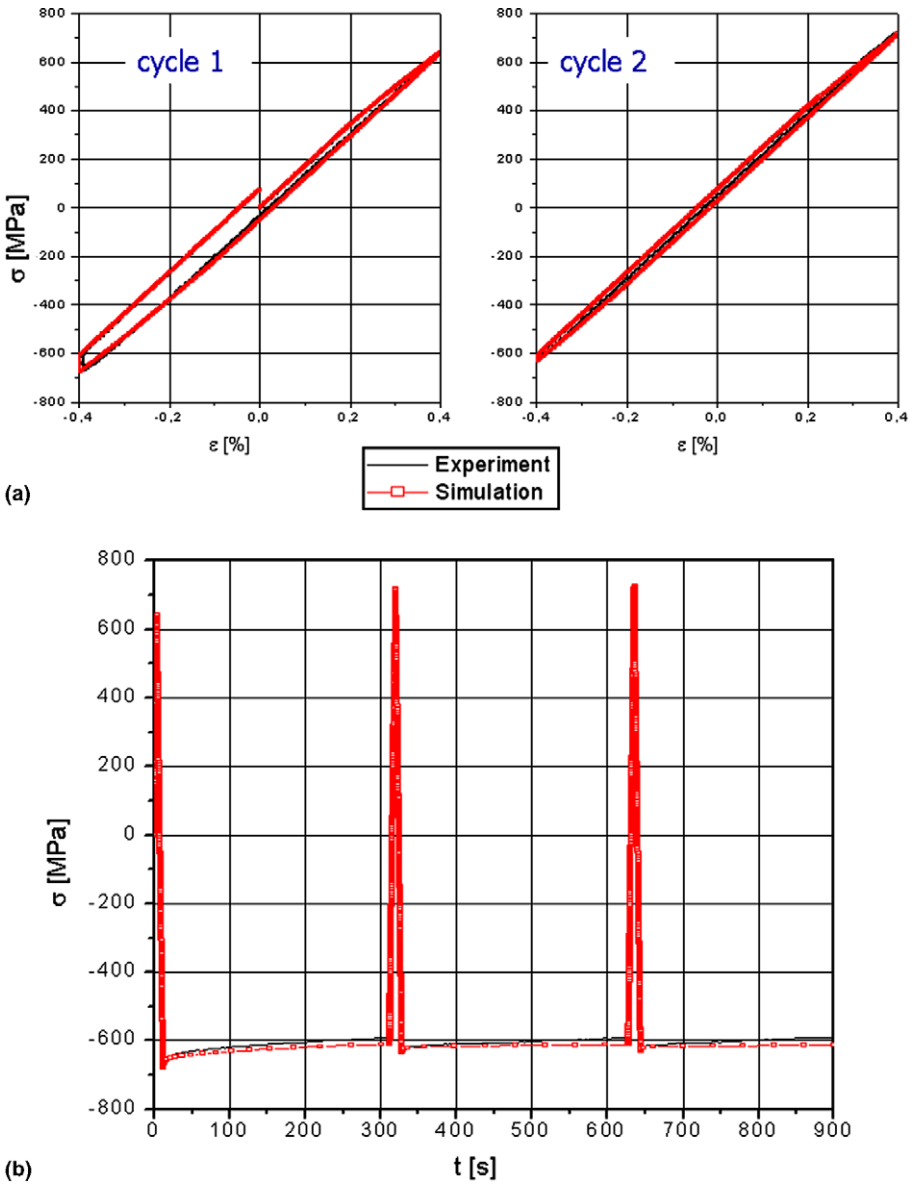

Fig. 7. Simulation of the deformation behaviour in a cyclic test with relaxation hold-times at 560 °C for the verification of the model: hysteresis loops of the first two cycles (above) and stress as function of time (below).

consumption D, $0 \leq D \leq 1$. The following lifetime rule has been used:

$$\frac{dD}{dt} = \left(\frac{r_{eq}}{A}\right)^{m_l} \left(\frac{\dot{p}}{\dot{p}_0}\right)^{n_l} \dot{p}_0; \quad r_{eq} = \sqrt{\frac{3}{2}}\,\|S\|; \tag{11}$$

where r_{eq} is the Mises equivalent stress, $\dot{p}$ the inelastic Mises equivalent strain-rate as defined in Eq. (7) and $\dot{p}_0$ is a normalisation constant. The material parameters A and m_l describe the stress-dependence of the lifetime behaviour. An influence of the mean stress of a cycle is taken into account automatically by the fact that a stress process, which is non-symmetric to the zero-point in the stress space during a cycle, moves for the same stress range as in a symmetric process at higher stress magnitudes, nevertheless. And these stresses are evaluated in the lifetime rule (11) by $m_l > 1$ as disproportionately high damaging compared to lower stress magnitudes. The parameter n_l describes the time-dependence of the lifetime: for rate-independent behaviour n_l is equal to 1, n_l equal to zero means that a fully time-dependent lifetime behaviour is present. n_l was found to be positive but significantly lower than 1 for the investigated high temperature loading.

The parameters A and m_l have been determined from LCF tests with strain-rates of $10^{-3}\ s^{-1}$ and without hold-times. The parameter n_l has been identified by the influence of hold-times in LCF tests on the lifetime behaviour. The cycles-to-failure N_f have been calculated by the formula

$$N_f = 1/(\Delta D)_s; \tag{12}$$

where $(\Delta D)_s$ is the lifetime consumption within one stabilised cycle.

The investigated specimens had a diameter of 6.5 mm in the gauge length. The cycles-to-failure of the LCF experiments have been determined at 2% stress drop in tension after the range of saturation.

The simulations of the experimentally determined lifetimes are given in Fig. 8. The lifetimes of the LCF tests with strain-rates of 10^{-4} and 10^{-3} s^{-1} represent a verification of the lifetime model: all simulated cycles-to-failure are within a factor of 2 with respect to the experimental ones.

For the chosen extrusion examples, the simulations led to maximum lifetime consumption in the region of relatively high both temperature and equivalent stresses (Fig. 9). During extrusion, the equivalent stress and temperature maxima are not located at exactly the same place in the liner. However, the largest accumulated damage occurs in regions that exhibit maximum overlapping temperature and equivalent stress loading. To compare the extrusion of aluminium and copper alloys, different billet temperatures have been considered in the simulations, whereas the radial stress boundary conditions have not been changed. This should be tolerable because despite temperatures are very different for aluminium and copper extrusion, the extrusion pressure and hence the radial stres-

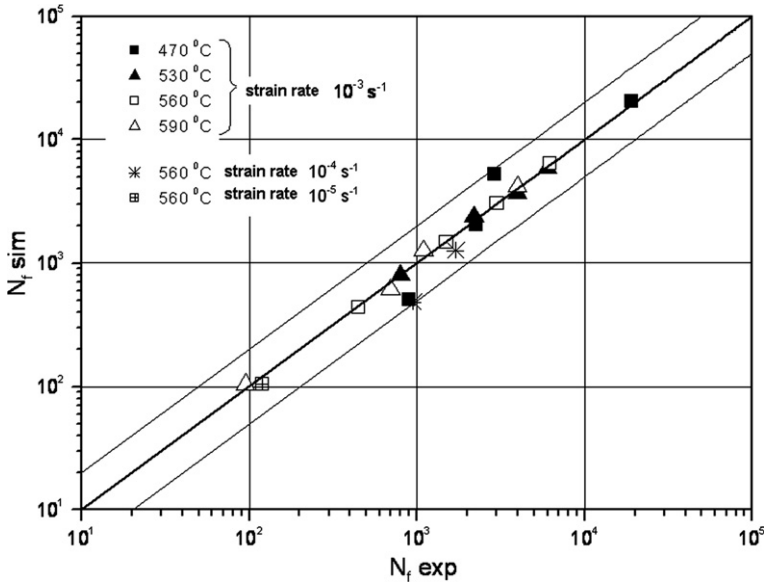

Fig. 8. Cycles-to-failure in experiment and simulation for different temperatures and strain-rates.

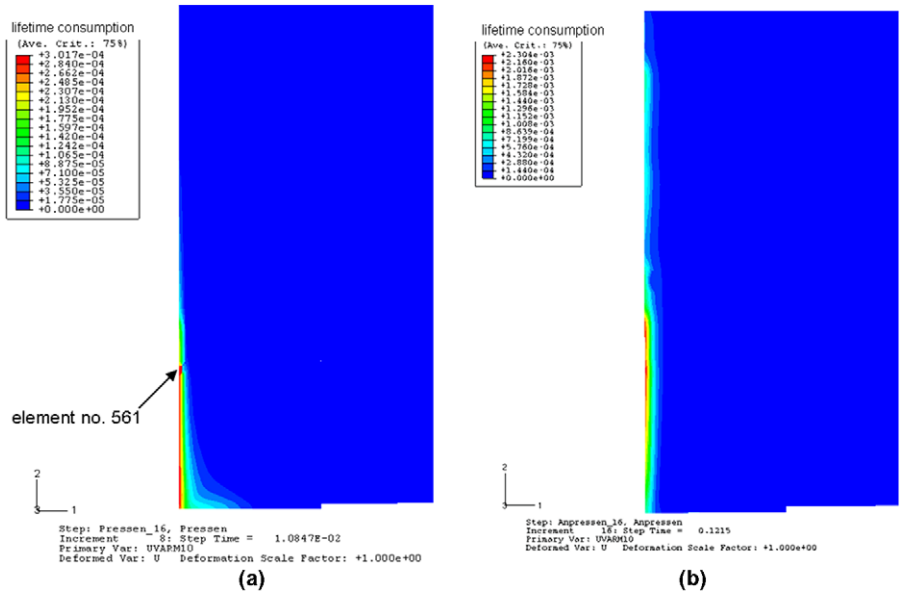

Fig. 9. Lifetime consumption distribution after the 15th cycle for both aluminium (a) and copper (b) extrusion (zoomed section with height of 200 mm). The arrow marked element (no. 561) has been compared related to the lifetime consumption for aluminium as well as copper extrusion.

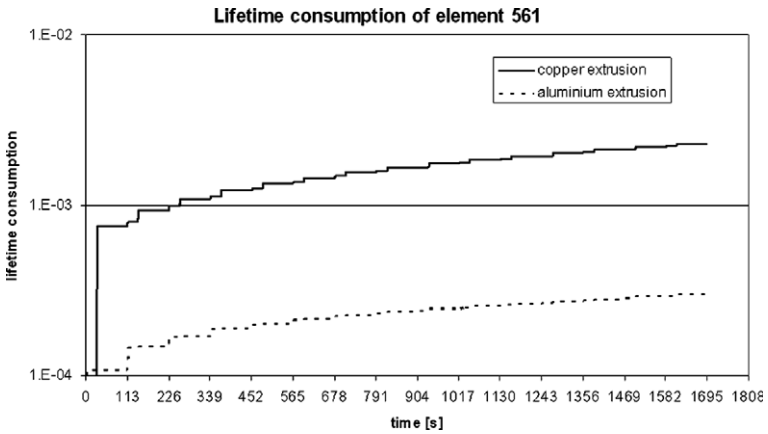

Fig. 10. Lifetime consumption over 15 extrusion cycles for one selected element in the damaged area of the liner. Comparison of aluminium and copper extrusion.

ses at the inner diameter of the liner are very similar comparing easily, medium and hard extrudable aluminium and copper alloys [8]. Fig. 10 depicts the lifetime consumption evolution with time for 15 extrusion cycles. For copper extrusion with its higher temperatures compared to aluminium extrusion, the lifetime consumption increments are higher at a factor of approx. 6.4. The calculated cycles-to-failure of the liner are 42,500 and 6600 for aluminium and copper extrusion, respectively. These results seem to be reasonable in comparison to real lifetime of aluminium as well as copper extrusion containers.

3. Conclusions and outlook

A thermo-viscoplastic constitutive model for the calculation of inelastic strains due to creep-fatigue loads in extrusion tools made of hot work steels has been presented.

With respect to the modelling of the deformation behaviour it has been found that the material parameters of static recovery of a viscoplastic model can be determined from a long-term stress-relaxation period where several magnitudes of the inelastic strain-rate occur which decrease with the decreasing magnitude of the stress-rate.

Furthermore, a fatigue lifetime rule for complex multiaxial loading is proposed that is independent of single loading parameters to describe an entire cycle. Instead this lifetime rule evaluates the total damage in each time increment and, thus, can easily be implemented in a material sub-routine for finite element analysis of structures just as an evolution equation for an additional internal variable, the lifetime consumption.

As an example, the lifetime of a liner during aluminium as well as copper extrusion has been predicted. Therefore the extrusion process has been simulated in order to get both the temperature and radial stress boundary conditions for a subsequent cyclic simulation of the temperature and stress evolution in the container. Here, both the chosen constitutive model and the time incremental lifetime rule have been coupled to the FEM model. Due to the higher applied temperatures during copper extrusion, the cycles-to-failure appeared to be lower with ca. 1 order of magnitude in comparison to aluminium extrusion.

In further calculations, an additional cooling system of the container for a more homogeneous temperature distribution shall be simulated, as well as the damage of the extrusion dies will be investigated. The calculated temperature and stress distribution will be compared to measured values with the help of an extrusion test device. Finally, both the impact of temperature and press speed changes on tools lifetime shall be analysed and different hot work tool steels will be compared related to lifetime.

Acknowledgement

The authors would like to thank very much the group of Dr. Ing. Klingelhöffer of the Division V.2 "Mechanical Behaviour of Materials" (head: Dr.-Ing. Skrotzki) of the Federal Institute for Materials Research and Testing (BAM) for performing the tests and Böhler Edelstahl GmbH for the financial support.

References

[1] W. Mitter, K. Haberfellner, R. Danzer, C. Stickler, HTM 52 (1997) 253–258.
[2] V. Wieser, C. Sommitsch, K. Haberfellner, P. Lehofer, in: ET'04 – Proceedings of the 8th International Aluminium Extrusion Technology Seminar, 2004, Kissimmee, Florida.
[3] S. Majumdar, P.S. Maiya, J. Eng. Mater. Technol 102 (1980) 159–167.
[4] A.S. Krausz, K. Krausz (Eds.), Unified Constitutive Laws of Plastic Deformation, Academic Press, 1996.
[5] J. Lemaitre, J.-L. Chaboche, Mechanics of Solid Materials, Cambridge University Press, 1990.
[6] J.-L. Chaboche, J. Appl. Mech. 60 (1993) 813–821.
[7] J. Olschewski, R. Sievert, A. Bertram, et al., in: Y. Hosoi (Ed.), Aspects of High Temperature Deformation and Fracture in Crystalline Materials (JIMIS-7), The Japan Institute of Metals, Nagoya, 1993, pp. 641–648.
[8] G. Sauer, A. Ames, Rezipienten, in: M. Bauser, G. Sauer, K. Siegert (Eds.), Strangpressen, Aluminium-Verlag, Düsseldorf, 2001, pp. 742–794, 2. Auflage.

[9] H. Frenz, J. Meersmann, J. Ziebs, H.-J. Kühn, R. Sievert, J. Olschewski, Mater. Sci. Eng. A 230 (1997) 49–57.
[10] O. Watanabe, S.N. Atluri, Int. J. Plasticity 2 (1986) 37–57.
[11] B. Ilschner, Hochtemperatur-Plastizität, Springer-Verlag, 1973.
[12] E. Krempl, Int. J. Plasticity 17 (2001) 1419–1436.
[13] J.-L. Chaboche, F. Gallerneau, Fatigue Fract. Eng. Mater. Struct. 24 (2001) 405–418.
[14] R. Danzer, Z. Metallkunde 78 (1987) 19–31.
[15] J.P. Sermage, J. Lemaitre, R. Desmorat, Fatigue Fract. Eng. Mater. Struct. 23 (2000) 241–252.
[16] N.-M. Yeh, E. Krempl, in: D.L. McDowell, R. Ellis (Eds.), Advances in Multiaxial Fatigue, ASTM STP, Philadelphia, 1993, pp. 107–109.
[17] V. Levkovitch, R. Sievert, B. Svendsen, in: P. Portella et al. (Eds.), Proc. Fifth International Conference on Low Cycle Fatigue (LCF 5), Deutscher Verband für Materialforschung und - prüfung (DVM), Berlin, 2004, pp. 415–420.